Odd-Parity Spin-Triplet Superconductivity in Centrosymmetric Antiferromagnetic Metals

Seung Hun Lee,[1,2,3] Hong Chul Choi,[1] and Bohm-Jung Yang[1,2,3,*]
[1]Center for Correlated Electron Systems, Institute for Basic Science (IBS), Seoul 08826, Korea
[2]Department of Physics and Astronomy, Seoul National University, Seoul 08826, Korea
[3]Center for Theoretical Physics (CTP), Seoul National University, Seoul 08826, Korea

(Received 28 June 2020; revised 30 October 2020; accepted 14 January 2021; published 10 February 2021)

We propose a route to achieve odd-parity spin-triplet (OPST) superconductivity in metallic collinear antiferromagnets with inversion symmetry. Owing to the existence of hidden antiunitary symmetry, which we call the effective time-reversal symmetry (eTRS), the Fermi surfaces of ordinary antiferromagnetic metals are generally spin degenerate, and spin-singlet pairing is favored. However, by introducing a local inversion symmetry breaking perturbation that also breaks the eTRS, we can lift the degeneracy to obtain spin-polarized Fermi surfaces. In the weak-coupling limit, the spin-polarized Fermi surfaces constrain the electrons to form spin-triplet Cooper pairs with odd parity. Interestingly, all the odd-parity superconducting ground states we obtained host nontrivial band topologies manifested as chiral topological superconductors, second-order topological superconductors, and nodal superconductors. We propose that double perovskite oxides with collinear antiferromagnetic or ferrimagnetic ordering, such as $SrLaVMoO_6$, are promising candidate systems where our theoretical ideas can be applied to.

DOI: 10.1103/PhysRevLett.126.067001

Introduction.—Magnetism and superconductivity are two representative quantum mechanical phenomena arising from spontaneous symmetry breaking. For decades, not only the individual phenomenon but also the interplay between them has been a central topic in condensed matter physics. Especially, motivated by the observation that the superconducting region usually appears near the magnetic quantum critical point [1–3], the pairing instability mediated by critical spin fluctuations has been extensively studied [1–11]. On the other hand, compared to the critical fluctuation driven superconductivity, the nature of the superconducting phase coexisting with stable magnetism has received relatively less attention [12–18]. However, various materials that exhibit magnetism and superconductivity simultaneously have been reported such as heavy fermion superconductors [19–29], iron-based superconductors [30–32], twisted double bilayer graphene [33–35], etc. Considering that magnetism strongly modifies the normal state symmetry, which in turn constrains possible pairing channels, coexisting magnetism and superconductivity has a great potential to realize unconventional superconductivity.

In fact, the structure of Cooper pairs can be significantly affected by magnetic ordering. For example, in ferromagnets, there is no Kramers degeneracy at general k points due to spin splitting, and the Fermi surface is spin polarized. Therefore, in the weak coupling limit where the spin-splitting energy is bigger than the pairing energy scale, Cooper pairs must be formed by equal-spin electrons, and the spin part of their wave function must be a triplet [36]. On the other hand, a collinear antiferromagnetic (AFM) ordering constrains Cooper pairs in a different manner [37–39]. Since a collinear AFM ordering preserves an *effective* time-reversal $\tilde{\Theta}$ symmetry (eTRS), defined as time-reversal operation Θ followed by a half lattice translation $t_{1/2}$ [37–39], if the system possesses additional inversion P symmetry, the Kramers degeneracy at general k points remains unlifted (see Fig. 1), unlike in ferromagnets [40]. Dominant spin-singlet pairing reported for several AFM superconductors [12,13] in earlier studies can be understood in this way. Therefore, to achieve stable spin-triplet pairing in the AFM system as in ferromagnetic systems, it is necessary to break the eTRS.

In this Letter, we propose a way to realize odd-parity spin-triplet (OPST) superconductivity in two-dimensional (2D) centrosymmetric collinear antiferromagnets. Here, the central idea is to introduce a perturbation that breaks local inversion symmetry between neighboring sites while keeping the inversion about a lattice site, such as staggered potential (SP) or antisymmetric spin-orbit coupling (ASOC) [41–43]. SP can arise when the sublattices are occupied by different magnetic ions while ASOC can generally appear in layered perovskite materials with rotation distortions of oxygen octahedra. Since SP or ASOC makes the sublattices inequivalent, eTRS is also broken [39]. Thus, in the presence of SP or ASOC, the Fermi surface of the AFM system becomes spin split, so that spin-triplet pairing can be predominant as in ferromagnets. Furthermore, it is found that the OPST pairing drives the AFM system with SP to be one of the following

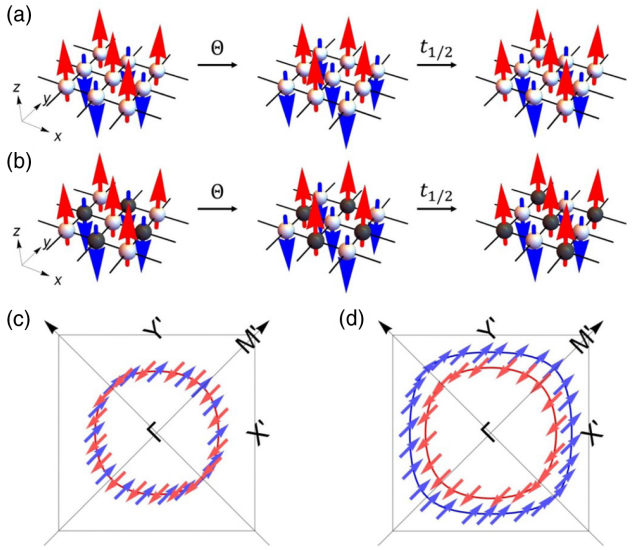

FIG. 1. (a) A two-dimensional (2D) collinear antiferromagnet invariant under the effective time-reversal symmetry $\tilde{\Theta} = t_{1/2}\Theta$. (b) A 2D collinear antiferromagnet with staggered sublattice potential $\epsilon_{\rm sp}$, which breaks $\tilde{\Theta}$. The atoms with different on-site potential energies ($\epsilon_{\rm sp} \neq 0$) are distinguished by white and gray colors. (c) The spin-degenerate Fermi surface when $\epsilon_{\rm sp} = 0$. (d) Similar figure as (c) when $\epsilon_{\rm sp} \neq 0$, where the Fermi surfaces are spin polarized.

topological superconductors (TSCs): a chiral (spin-chiral) TSC with a nonzero Chern (spin-Chern) number, and a nodal TSC. The chiral TSC is robust against the inclusion of spin-orbit coupling (SOC) while the stability of the spin-chiral TSC against SOC requires mirror or spin-reflection symmetry. Interestingly, once the mirror or spin-reflection symmetry is broken, the spin-chiral TSC with SOC turns into a second-order TSC.

Model.—We consider a tight-binding model for a Néel ordered antiferromagnet on a square lattice. For simplicity, we include up to the nearest-neighbor (NN) hoppings in our model Hamiltonian $\hat{H} = \sum_k \mathbf{c}_{\mathbf{k}}^\dagger \mathcal{H}_{\rm nn}(\mathbf{k})\mathbf{c}_{\mathbf{k}}$, where $\mathbf{c}_{\mathbf{k}}^\dagger = (c_{\mathbf{k}A\uparrow}^\dagger, c_{\mathbf{k}B\uparrow}^\dagger, c_{\mathbf{k}A\downarrow}^\dagger, c_{\mathbf{k}B\downarrow}^\dagger)$, and $\mathcal{H}_{\rm nn}(\mathbf{k}) = 2t(\cos k_x + \cos k_y)\sigma_0\tau_x \equiv \epsilon_{\rm nn}(\mathbf{k})\sigma_0\tau_x$. σ and τ are Pauli matrices representing the spin ($\uparrow$, $\downarrow$) and sublattice (A, B) degrees of freedom, respectively. Then, to describe the effect of the collinear AFM ordering, we introduce a mean-field approximated exchange coupling term $-\mathbf{m}\cdot\boldsymbol{\sigma}\tau_z$ so that the Hamiltonian becomes

$$\mathcal{H}_0(\mathbf{k}) = \epsilon_{\rm nn}(\mathbf{k})\sigma_0\tau_x - \mathbf{m}\cdot\boldsymbol{\sigma}\tau_z, \tag{1}$$

whose energy spectrum is doubly degenerate at every k point in the Brillouin zone due to the inversion $P = \sigma_0\tau_0$ and eTRS $\tilde{\Theta} = i\sigma_y\tau_x K$ [44].

However, if we take into account SP or ASOC in the form of $\epsilon_{\rm sp}\sigma_0\tau_z$ or $\sum_{i=x,y,z} 2v_i(\cos k_x + \cos k_y)\sigma_i\tau_y \equiv \boldsymbol{\epsilon}_{\rm asoc}(\mathbf{k})\cdot\boldsymbol{\sigma}\tau_y$, respectively, which breaks the inversion between neighboring sites while keeping the inversion about a lattice site, we immediately find that eTRS is broken and spin degeneracy is lifted. For the rest of this work, we study the universal properties of the AFM superconductivity considering SP only. In the case of ASOC, since the details of $\mathbf{v}$ significantly affect the symmetry of the system, more specific information from materials is necessary to examine its influence. The final form of the normal state Hamiltonian is then given by $\mathcal{H}(\mathbf{k}) = \mathcal{H}_0(\mathbf{k}) + \epsilon_{\rm sp}\sigma_0\tau_z$. Figure 1 shows spin expectation values of the eigenstates of $\mathcal{H}(\mathbf{k})$ on the Fermi surfaces for $\mathbf{m} = (m, 0, 0)$ without $\epsilon_{\rm sp}$ [Fig. 1(c)] and with a finite $\epsilon_{\rm sp}$ [Fig. 1(d)]. In contrast to the spin-degenerate Fermi surface in Fig. 1(c), each Fermi surface in Fig. 1(d) is indeed spin polarized.

Group theoretical classification of pairing functions.—To describe superconductivity, we consider short-ranged density-density interactions

$$H_{\rm int} = -U\int d\mathbf{r}\sum_{l=A,B} n_{l\uparrow}(\mathbf{r})n_{l\downarrow}(\mathbf{r}) - V\int d\mathbf{r}\sum_{l\neq l'}\sum_{\sigma\sigma'}\sum_i n_{l\sigma}(\mathbf{r})n_{l'\sigma'}(\mathbf{r}+\boldsymbol{\delta}_i), \tag{2}$$

where U and V denote the on-site and NN-site attractive interactions, respectively. We take the Nambu basis in the form of $\Psi_{\mathbf{k}}^\dagger = (\mathbf{c}_{\mathbf{k}}^\dagger, \mathbf{c}_{-\mathbf{k}})$, and write the Bogoliubov–de Gennes (BdG) Hamiltonian as $\sum_{\mathbf{k}} \Psi_{\mathbf{k}}^\dagger \mathcal{H}_{\rm BdG}(\mathbf{k})\Psi_{\mathbf{k}}$ with

$$\mathcal{H}_{\rm BdG}(\mathbf{k}) = \begin{pmatrix} \mathcal{H}(\mathbf{k}) - \mu & \Delta(\mathbf{k}) \\ \Delta^\dagger(\mathbf{k}) & -\mathcal{H}^T(-\mathbf{k}) + \mu \end{pmatrix}, \tag{3}$$

where μ and $\Delta(\mathbf{k})$ denote the chemical potential and mean-field pairing interaction, respectively. In general, it is able to express the pairing function in the basis of $\tilde{\sigma}_i\tau_j$'s as $\Delta(\mathbf{k}) = \sum_{ij} f_{ij}(\mathbf{k})\tilde{\sigma}_i\tau_j$, where $\tilde{\sigma}_i \equiv \sigma_i(i\sigma_y)$. Because of the fermionic statistics, $\Delta(\mathbf{k})$ must satisfy $\Delta(\mathbf{k}) = -\Delta^T(-\mathbf{k})$. Following the Sigrist-Ueda method [45], we classify possible pairing functions that can arise from $H_{\rm int}$ by the irreducible representations (IRs) of the point group for two representative collinear AFM structures with high symmetry: out-of-plane AFM (O-AFM) ordering along [001] direction, and in-plane AFM (I-AFM) ordering along [100] direction. In the presence of the O-AFM (I-AFM) ordering $\mathbf{m} = (0, 0, m)$ [$(m, 0, 0)$] together with SP, the system belongs to C_{4h}^z (C_{2h}^x) point group, whose principal axis is the z axis (x axis). Hereafter, we denote the γth gap function that belongs to the Γ IR by $[f(\mathbf{k})\sigma\tau]_\gamma^\Gamma$. As each gap function represents an independent pairing channel, we define a corresponding order parameter as $\Delta_\gamma^\Gamma \equiv -V_\gamma^\Gamma\langle\mathbf{c}_{\mathbf{k}}^T[f(\mathbf{k})\sigma\tau]_\gamma^{\Gamma*}\mathbf{c}_{\mathbf{k}}\rangle$, where $V_\gamma^\Gamma = U(V)$ for intra-sublattice (intersublattice) channels. Then a general expression of a pairing potential that belongs to the Γ representation reads $\Delta^\Gamma(\mathbf{k}) = \sum_\gamma \Delta_\gamma^\Gamma[f(\mathbf{k})\sigma\tau]_\gamma^\Gamma$ and the

TABLE I. Superconducting gap structures (GS) of various pairing channels. FG indicates that the bulk is fully gapped. NP indicates that pairs of nodal points appear. NG means there is no superconducting gap.

AFM	Δ_γ^Γ	$[f(\mathbf{k})\sigma\tau]_\gamma^\Gamma$	GS
O-AFM	$\Delta_1^{A_u}$	$\sin k_x\tilde{\sigma}_x\tau_x + \sin k_y\tilde{\sigma}_y\tau_x$	FG
	$\Delta_2^{A_u}$	$\sin k_x\tilde{\sigma}_y\tau_x - \sin k_y\tilde{\sigma}_x\tau_x$	FG
	$\Delta_1^{B_u}$	$\sin k_x\tilde{\sigma}_x\tau_x - \sin k_y\tilde{\sigma}_y\tau_x$	FG
	$\Delta_2^{B_u}$	$\sin k_x\tilde{\sigma}_y\tau_x + \sin k_y\tilde{\sigma}_x\tau_x$	FG
	Others		NG
I-AFM	$\Delta_1^{A_u}$	$\sin k_y\tilde{\sigma}_y\tau_x$	NP
	$\Delta_2^{A_u}$	$\sin k_y\tilde{\sigma}_z\tau_x$	NP
	$\Delta_1^{B_u}$	$\sin k_x\tilde{\sigma}_y\tau_x$	NP
	$\Delta_2^{B_u}$	$\sin k_x\tilde{\sigma}_z\tau_x$	NP
	Others		NG

corresponding BdG Hamiltonian is denoted by $\mathcal{H}_{\mathrm{BdG}}^\Gamma(\mathbf{k})$. In Table I, we summarize the result of the group theoretical classification and the gap structure analysis for various Γ's and γ's.

Referring to Table I, only the gap functions in the A_u and B_u IRs can open superconducting gap on the Fermi surfaces in the weak-pairing limit, while others cannot. It means that, only OPST channels in the A_u and B_u IRs can contribute to the superconducting instability, for both the O-AFM and the I-AFM cases. The gap structures of $\Delta^\Gamma(\mathbf{k})$'s when there are two Fermi surfaces around the Γ point are visualized in Fig. 2.

Mean field theory and Ginzburg-Landau free energy.—To determine the leading instability and find the exact forms of $\Delta^\Gamma(\mathbf{k})$'s in the superconducting states, we proceed to solve the linearized gap equation. The free energy of the system is given by

$$F = \frac{1}{V}\sum_\gamma |\Delta_\gamma^\Gamma|^2 - \frac{1}{\beta}\sum_N\sum_{\mathbf{k}n}\ln\left[\omega_N^2 + \xi_n^2(\mathbf{k})\right], \quad (4)$$

where ω_N is the Nth fermionic Matsubara frequency, and $\xi_n(\mathbf{k})$ is the negative eigenvalue of $\mathcal{H}_{\mathrm{BdG}}^\Gamma(\mathbf{k})$ with nth smallest absolute value. The range of the summation over n changes depending on μ, because we are interested only in the energy bands which cross the Fermi level. Thus, we consider three different cases: case (i) $\min\lambda_-(\mathbf{k}) < |\mu| < \min\lambda_+(\mathbf{k})$, case (ii) $\min\lambda_+(\mathbf{k}) < |\mu| < \max\lambda_-(\mathbf{k})$, and case (iii) $\max\lambda_-(\mathbf{k}) < |\mu| < \max\lambda_+(\mathbf{k})$, where $\lambda_\pm = \sqrt{(m \pm \epsilon_{\mathrm{sp}})^2 + \epsilon_{\mathrm{nn}}^2(\mathbf{k})}$. Here $\min\lambda$ ($\max\lambda$) denotes the minimum (maximum) value of λ. In case (i) [case (iii)], only ξ_1 (ξ_2) is included in the summation, while in case (ii), ξ_1 and ξ_2 are included [see Fig. 2(d)].

Using polar forms of the complex numbers $\Delta_\gamma^\Gamma = |\Delta_\gamma^\Gamma|e^{i\theta_\gamma^\Gamma}$, the equilibrium conditions are given by

$$\frac{\partial F}{\partial\theta_\gamma^\Gamma} = -\frac{1}{\beta}\sum_N\sum_{\mathbf{k}n}\frac{\partial\xi_n^2(\mathbf{k})/\partial\theta_\gamma^\Gamma}{\omega_N^2 + \xi_n^2(\mathbf{k})} = 0, \quad (5)$$

$$\frac{\partial F}{\partial|\Delta_\gamma^\Gamma|} = \frac{2}{V}|\Delta_\gamma^\Gamma| - \frac{1}{\beta}\sum_N\sum_{\mathbf{k}n}\frac{\partial\xi_n^2(\mathbf{k})/\partial|\Delta_\gamma^\Gamma|}{\omega_N^2 + \xi_n^2(\mathbf{k})} = 0, \quad (6)$$

where Eq. (6) is the so-called linearized gap equation. For $\Gamma = A_u$ and B_u, our model gives that both $\partial F/\partial\theta_1^\Gamma$ and $\partial F/\partial\theta_2^\Gamma$ are proportional to $|\Delta_1^\Gamma||\Delta_2^\Gamma|\cos(\theta_1^\Gamma - \theta_2^\Gamma)$, implying that the free energy is minimized when either one of the two order parameters vanishes, or $\cos(\theta_1^\Gamma - \theta_2^\Gamma) = 0$ (i.e., $|\Delta_1^\Gamma| = \pm i|\Delta_2^\Gamma|$). However, when $|\Delta_1^\Gamma| = \pm i|\Delta_2^\Gamma|$, the pairing interaction can induce the gap only on one of the two possible Fermi surfaces. Thus, $(\Delta_1^\Gamma, \Delta_2^\Gamma) = (\Delta, 0)$ or $(0, \Delta)$ is favored for case (ii), while one of the two solutions $(\Delta_1^\Gamma, \Delta_2^\Gamma) = \Delta(i, 1)$ or $\Delta(1, i)$ is favored for cases (i) and (iii). The transition temperature for each case can be calculated by solving Eq. (6). However, we note that our model does not have enough anisotropy to differentiate the transition temperatures of the superconducting states in the A_u and B_u IRs, unless extra perturbations allowed by the symmetry enter the Hamiltonian. For example, in the I-AFM case, the two representations can be distinguished if the hopping amplitudes along the x and y directions are different.

Topological superconductivity (TSC).—Odd-parity pairings play a key role in TSC in centrosymmetric systems [46–48]. Here we study the topological properties of the OPST superconducting states in the A_u and B_u IRs, obtained above. Both the O-AFM and the I-AFM superconductors belong to the D symmetry class in the Altland-Zirnbauer (AZ) classification table [49–52]. However, the

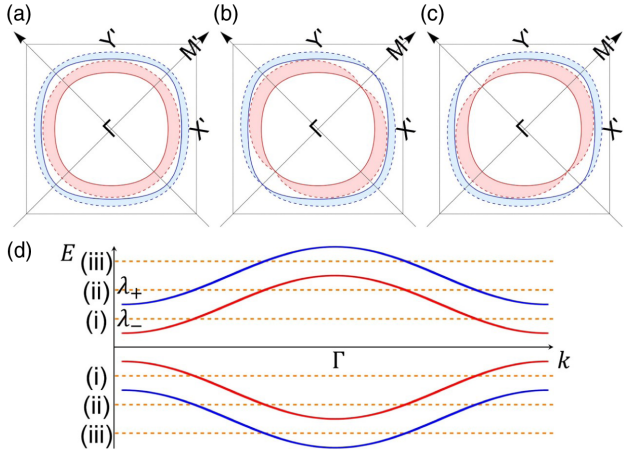

FIG. 2. The superconducting gap structures for (a) $\Delta^{A_u}(\mathbf{k})$ and $\Delta^{B_u}(\mathbf{k})$ of the O-AFM, (b) $\Delta^{A_u}(\mathbf{k})$ of the I-AFM, (c) $\Delta^{B_u}(\mathbf{k})$ of the I-AFM. The red and blue solid lines represent the Fermi surfaces. The distance between a solid line and a dashed line with the same color represents the size of the relevant superconducting gap on the Fermi surface. (d) Schematic figure for cases (i), (ii), and (iii) with different Fermi levels shown together with the energy spectrum of the normal state, $\pm\lambda_\pm(\mathbf{k})$.

quasiparticle spectrum of the O-AFM superconductor is fully gapped, while that of the I-AFM superconductor has gapless nodes. Thus, we treat the two cases separately.

To check the topological properties of the O-AFM superconductors, we calculate the Wilson loop eigenvalue spectrum of the occupied bands of $\mathcal{H}^{\Gamma}_{\mathrm{BdG}}(\mathbf{k})$ [53,54]. Since the spin-up and spin-down sectors of $\mathcal{H}^{\Gamma}_{\mathrm{BdG}}(\mathbf{k})$ are totally decoupled, $\mathcal{H}^{\Gamma}_{\mathrm{BdG}}(\mathbf{k})$ can be reduced into two blocks as

$$\mathcal{H}^{\Gamma}_{\mathrm{BdG}}(\mathbf{k}) = \begin{pmatrix} \mathcal{H}^{\Gamma,\uparrow\uparrow}_{\mathrm{BdG}}(\mathbf{k}) & 0 \\ 0 & \mathcal{H}^{\Gamma,\downarrow\downarrow}_{\mathrm{BdG}}(\mathbf{k}) \end{pmatrix}. \tag{7}$$

We find that $\mathcal{H}^{\Gamma,\downarrow\downarrow}_{\mathrm{BdG}}(\mathbf{k})$ [$\mathcal{H}^{\Gamma,\uparrow\uparrow}_{\mathrm{BdG}}(\mathbf{k})$] has a nontrivial winding in its Wilson loop spectrum in case (i) [case (iii)], while the other block does not. It indicates that the occupied bands of $\mathcal{H}^{\Gamma,\downarrow\downarrow}_{\mathrm{BdG}}(\mathbf{k})$ ($\mathcal{H}^{\Gamma,\uparrow\uparrow}_{\mathrm{BdG}}(\mathbf{k})$) have a nonzero Chern number. On the other hand, both blocks carry finite Chern numbers but with opposite signs in case (ii), making the total Chern number of the system zero. This result agrees well with the Fu-Berg-Sato criteria for diagnosing band topology in centrosymzmetric systems [46,47]. We note that $\mathcal{C}^{A_u,\sigma\sigma}_{\mathrm{BdG}} = -\mathcal{C}^{B_u,\sigma\sigma}_{\mathrm{BdG}}$, where $\mathcal{C}^{\Gamma,\sigma\sigma}_{\mathrm{BdG}}$ denotes the Chern number carried by the occupied bands of $\mathcal{H}^{\Gamma,\sigma\sigma}_{\mathrm{BdG}}$ ($\sigma\sigma = \uparrow\uparrow$ or $\downarrow\downarrow$). Corresponding to the nontrivial bulk topology, gapless modes appear on the edges of the system [55–60]. To confirm this, we have performed the finite-size tight-binding model calculation for the system in a ribbon geometry. Figure 3(a) displays the result for $\Gamma = A_u$ in case (ii). In fact, the two blocks in Eq. (7) are nothing but the mirror M_z invariant sectors with the eigenvalues ± 1, respectively, where M_z: $(x, y, z) \to (x, y, -z)$. Thus, the case (ii) O-AFM superconducting state can be interpreted as a mirror Chern superconductor, whose $M_z = \pm 1$ eigensectors are analogous to chiral p-wave superconductors with the Chern number ± 1 [61]. If the system preserves the M_z symmetry, the above discussion is still valid even in the presence of SOC. When M_z is broken, the two edge channels of case (ii) superconductor mix and open a gap [Fig. 3(b)], leading to a second-order TSC protected by inversion symmetry [62,75–77].

In the I-AFM case, as $\Delta^{A_u}(\mathbf{k}) \propto \sin k_x$ [$\Delta^{B_u}(\mathbf{k}) \propto \sin k_y$], there are nodes at the points where the k_y (k_x) axis intersects the Fermi surfaces as shown in Fig. 1. However, these nodes can be pairwise annihilated by adding symmetry-preserving perturbations [see Fig. 3(c)], which give gapped bulk states. When the spin-reflection symmetry $S_x = i\sigma_x$ exists, as the spin-up and spin-down edge states are decoupled, the I-AFM superconductor becomes a spin-chiral (chiral) TSC for case (ii) [case (i) and (iii)], similar to the O-AFM cases. When S_x breaking SOC exists, the edge states of the spin-chiral TSC are gapped. Interestingly, the resulting gapped phase turns out to be a second-order TSC protected by inversion symmetry [75,76]. The edge states of various TSCs for I-AFM superconductors are shown in Fig. 3(c).

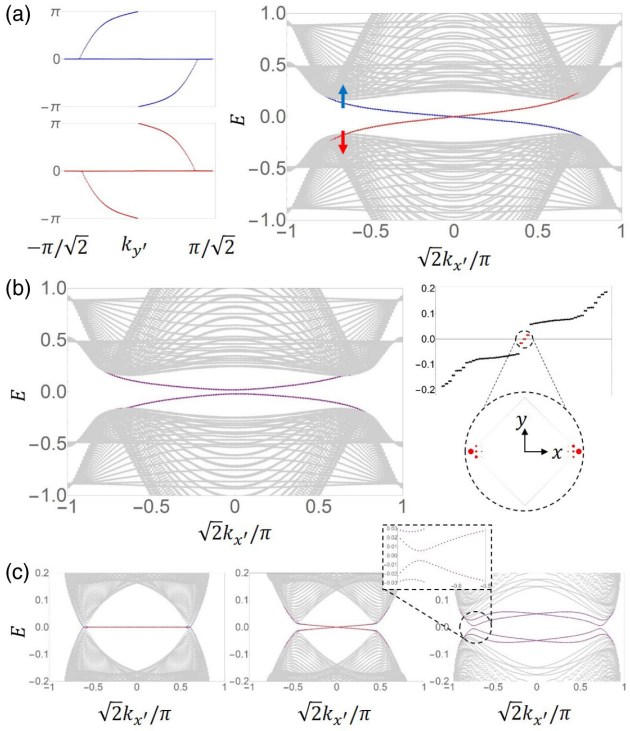

FIG. 3. (a) (Left) The Wilson loop eigenvalue spectra of $\mathcal{H}^{A_u,\uparrow\uparrow}_{\mathrm{BdG}}(\mathbf{k})$ (upper) and $\mathcal{H}^{A_u,\downarrow\downarrow}_{\mathrm{BdG}}(\mathbf{k})$ (lower) for the case (ii) O-AFM superconductor. The two block Hamiltonians have the opposite Chern numbers. (Right) Energy spectrum for an edge of a finite-size system with a ribbon geometry extended along $x'(1, 1, 0)$ direction while having a finite length along $y'(-1, 1, 0)$ direction. The chiral edge modes originate from spin-up (blue) and spin-down (red) bands. (b) (Left) Gapped edge spectrum due to the M_z breaking SOC. (Right) Corresponding zero-energy corner modes. (c) (Left) Energy spectrum of a ribbon geometry described in (a) for the case (ii) I-AFM superconductor. (Middle) Gapped bulk and gapless edge spectra after pair annihilation of bulk nodes. (Right) Gapped edge spectrum in the presence of SOC breaking spin-reflection symmetry. The parameter values used to generate this figure are $t = 0.667$, $m = 0.314$, $\epsilon_{\mathrm{sp}} = 0.2$, $\mu = -1.0$, and $\Delta = 0.1$. We take $3t/2 = 1$ as the energy unit.

Application to double perovskites.—We propose that a class of materials called double perovskites (DPs) with a formula $A_2BB'O_6$ [78] is a promising candidate where our theoretical idea can be tested. The DPs share the same lattice structure as conventional centrosymmetric perovskites. However, composed of two different species of transition metals B and B′, they can be seen as lattice systems with SP. Moreover, ASOC can also arise from rotations and tilts of oxygen octahedra in the DPs. The DPs have long been expected as candidates for exotic magnetic phases such as half-metallic AFMs [79–84] and metallic AFMs [85,86]. Especially, by first-principles calculations, we predict that a doped DP (C-type) $SrLaVMoO_6$ is a metallic compound whose nearest neighbor V and Mo sites have antiferromagnetically (or ferrimagnetically) ordered local spin moments (see Supplemental Material [62]).

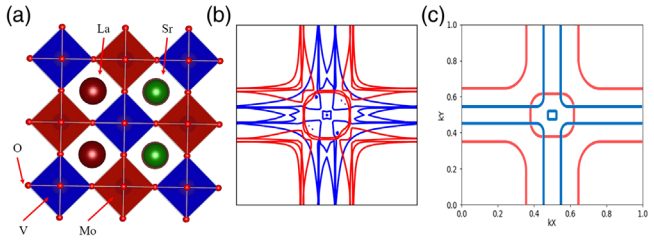

FIG. 4. (a) Lattice structure of the C-type $SrLaVMoO_6$. (b) The Fermi surfaces of the C-type $SrLaVMoO_6$ on $k_z = 0$ plane obtained by first-principles calculations. Red and blue lines denote spin-up and spin-down Fermi surfaces, respectively. (c) A schematic interpretation of the Fermi surfaces.

Figure 4 shows that the Fermi surfaces of $SrLaVMoO_6$ are spin split as expected. Since the layered structure of DPs is also available by partitioning the bulk crystal with organic cations [87], we anticipate that our model, the square lattice antiferromagnet with SP on its sublattices, can be realized in the DP compound like $SrLaVMoO_6$.

Conclusions.—We propose that 2D AFM metals with broken eTRS favors OPST superconducting states. As shown in the Supplemental Material [62], our mean field solutions are stable against RPA-type flucutations due to the spin anisotropy of AFM normal states. Also we confirmed that our OPST pairing is more stable than the Fulde-Ferrel-Larkin-Ovchinnikov (FFLO) pairing in the weak-pairing limit, especially when SP is large, as the FFLO pairing cannot open the gap at the Fermi surface (see Supplemental Material [62]). We believe that the superconductivity of AFM metals provides a promising platform for searching new types of TSCs protected by magnetic space group symmetries associated with the background magnetic ordering. Finally, we note that our OPST superconductivity of AFM metals is distinct from the superconductivity arising from local noncentrosymmetry in paramagnetic metals [41], and also from the parity-mixed spin-triplet superconductors featured in noncentrosymmetric antiferromagnets [13,15,88].

We thank Junyeong Ahn, Sungjoon Park, Yoonseok Hwang, and Se Young Park for helpful discussions. S. L. and B.-J. Y. were supported by the Institute for Basic Science in Korea (Grant No. IBS-R009-D1) and Basic Science Research Program through the National Research Foundation of Korea (NRF) (Grant No. 0426-20200003). H. C. C. was supported by Institute for Basic Science in Korea (IBS-R009-D1). This work was supported in part by the U.S. Army Research Office under Grant No. W911NF-18-1-0137.

*bjyang@snu.ac.kr

[1] L. Taillefer, Annu. Rev. Condens. Matter Phys. **1**, 51 (2010).
[2] N. Nagaosa, Science **275**, 1078 (1997).
[3] S. Sachdev, Science **336**, 1510 (2012).
[4] T. Kuwabara and M. Ogata, Phys. Rev. Lett. **85**, 4586 (2000).
[5] Z. Y. Meng, Y. B. Kim, and H.-Y. Kee, Phys. Rev. Lett. **113**, 177003 (2014).
[6] S. Sumita, T. Nomoto, and Y. Yanase, Phys. Rev. Lett. **119**, 027001 (2017).
[7] D. E. Almeida, R. M. Fernandes, and E. Miranda, Phys. Rev. B **96**, 014514 (2017).
[8] C. Setty, S. Bhattacharyya, A. Kreisel, and P. Hirschfeld, Nat. Commun. **11**, 523 (2019).
[9] D. Fay and J. Appel, Phys. Rev. B **22**, 3173 (1980).
[10] Y. Tada, S. Fujimoto, N. Kawakami, T. Hattori, Y. Ihara, K. Ishida, K. Deguchi, N. Sato, and I. Satoh, J. Phys. Conf. Ser. **449**, 012029 (2013).
[11] J. Ishizuka and Y. Yanase, Phys. Rev. B **98**, 224510 (2018).
[12] K. Machida, K. Nokura, and T. Matsubara, Phys. Rev. B **22**, 2307 (1980).
[13] S. Fujimoto, J. Phys. Soc. Jpn. **75**, 083704 (2006).
[14] M. V. Milovanović and S. Predin, Phys. Rev. B **86**, 195113 (2012).
[15] Y. Qi, L. Fu, K. Sun, and Z. Gu, Phys. Rev. B **102**, 245140 (2020).
[16] B. Powell, J. F. Annett, and B. Györffy, J. Phys. A **36**, 9289 (2003).
[17] A. K. C. Cheung and S. Raghu, Phys. Rev. B **93**, 134516 (2016).
[18] E. Kadzielawa-Major, M. Fidrysiak, P. Kubiczek, and J. Spałek, Phys. Rev. B **97**, 224519 (2018).
[19] R. Feyerherm, A. Amato, F. N. Gygax, A. Schenck, C. Geibel, F. Steglich, N. Sato, and T. Komatsubara, Phys. Rev. Lett. **73**, 1849 (1994).
[20] P. G. Pagliuso, C. Petrovic, R. Movshovich, D. Hall, M. F. Hundley, J. L. Sarrao, J. D. Thompson, and Z. Fisk, Phys. Rev. B **64**, 100503(R) (2001).
[21] G. Knebel, D. Aoki, D. Braithwaite, B. Salce, and J. Flouquet, Phys. Rev. B **74**, 020501(R) (2006).
[22] S. Saxena, P. Agarwal, K. Ahilan, F. Grosche, R. Haselwimmer, M. Steiner, E. Pugh, I. Walker, S. Julian, P. Monthoux *et al.*, Nature (London) **406**, 587 (2000).
[23] D. Aoki, A. Huxley, E. Ressouche, D. Braithwaite, J. Flouquet, J.-P. Brison, E. Lhotel, and C. Paulsen, Nature (London) **413**, 613 (2001).
[24] N. Huy, A. Gasparini, D. De Nijs, Y. Huang, J. Klaasse, T. Gortenmulder, A. de Visser, A. Hamann, T. Görlach, and H. V. Löhneysen, Phys. Rev. Lett. **99**, 067006 (2007).
[25] J. Linder, I. B. Sperstad, A. H. Nevidomskyy, M. Cuoco, and A. Sudbø, Phys. Rev. B **77**, 184511 (2008).
[26] A. Gasparini, Y. Huang, N. Huy, J. Klaasse, T. Naka, E. Slooten, and A. De Visser, J. Low Temp. Phys. **161**, 134 (2010).
[27] B. Wu, G. Bastien, M. Taupin, C. Paulsen, L. Howald, D. Aoki, and J.-P. Brison, Nat. Commun. **8**, 14480 (2017).
[28] S. Ran, C. Eckberg, Q.-P. Ding, Y. Furukawa, T. Metz, S. R. Saha, I.-L. Liu, M. Zic, H. Kim, J. Paglione *et al.*, Science **365**, 684 (2019).
[29] S. Sundar, S. Gheidi, K. Akintola, A. M. Côté, S. R. Dunsiger, S. Ran, N. P. Butch, S. R. Saha, J. Paglione, and J. E. Sonier, Phys. Rev. B **100**, 140502(R) (2019).
[30] S. Ikeda, Y. Tsuchiya, X.-W. Zhang, S. Kishimoto, T. Kikegawa, Y. Yoda, H. Nakamura, M. Machida, J. K.

Glasbrenner, and H. Kobayashi, Phys. Rev. B **98**, 100502 (R) (2018).
[31] X. Lu, N. Wang, H. Wu, Y. Wu, D. Zhao, X. Zeng, X. Luo, T. Wu, W. Bao, G. Zhang *et al.*, Nat. Mater. **14**, 325 (2015).
[32] D. K. Pratt, W. Tian, A. Kreyssig, J. L. Zarestky, S. Nandi, N. Ni, S. L. Bud'ko, P. C. Canfield, A. I. Goldman, and R. J. McQueeney, Phys. Rev. Lett. **103**, 087001 (2009).
[33] X. Liu, Z. Hao, E. Khalaf, J. Y. Lee, K. Watanabe, T. Taniguchi, A. Vishwanath, and P. Kim, Nature (London) **583**, 221 (2020).
[34] J. Y. Lee, E. Khalaf, S. Liu, X. Liu, Z. Hao, P. Kim, and A. Vishwanath, Nat. Commun. **10**, 5333 (2019).
[35] F. Wu and S. Das Sarma, Phys. Rev. B **101**, 155149 (2020).
[36] M. Sigrist, AIP Conf. Proc. **1162**, 55 (2009).
[37] R. Ramazashvili, Phys. Rev. Lett. **101**, 137202 (2008).
[38] R. Ramazashvili, Phys. Rev. B **79**, 184432 (2009).
[39] L. Šmejkal, R. González-Hernández, T. Jungwirth, and J. Sinova, arXiv:1901.00445.
[40] The combination of inversion symmetry and the eTRS is an antiunitary symmetry whose square is -1. Since the combined symmetry is local in the momentum space, it protects the Kramers degeneracy at any k point.
[41] M. H. Fischer, F. Loder, and M. Sigrist, Phys. Rev. B **84**, 184533 (2011).
[42] J. Goryo, M. H. Fischer, and M. Sigrist, Phys. Rev. B **86**, 100507(R) (2012).
[43] S. Hayami, H. Kusunose, and Y. Motome, Phys. Rev. B **97**, 024414 (2018).
[44] More rigorously, $\tilde{\Theta}_{\mathbf{k}} = t_{1/2}\Theta = ie^{i\mathbf{k}\cdot(\mathbf{a}/2)}\sigma_y\tau_x K$ and $\tilde{\Theta}_{\mathbf{k}}\mathcal{H}(\mathbf{k})\tilde{\Theta}_{\mathbf{k}}^{-1} = \mathcal{H}(-\mathbf{k})$, where $t_{1/2}$ and $\mathbf{a}$ denote the half translation operator and the lattice vector, respectively. But the extra phase factor coming from the translation by half the lattice vector is not important in this context, so we omit it and write $\tilde{\Theta}$ as $i\sigma_y\tau_x K$ from now on.
[45] M. Sigrist and K. Ueda, Rev. Mod. Phys. **63**, 239 (1991).
[46] L. Fu and E. Berg, Phys. Rev. Lett. **105**, 097001 (2010).
[47] M. Sato, Phys. Rev. B **81**, 220504(R) (2010).
[48] S. Nakosai, Y. Tanaka, and N. Nagaosa, Phys. Rev. Lett. **108**, 147003 (2012).
[49] A. Altland and M. R. Zirnbauer, Phys. Rev. B **55**, 1142 (1997).
[50] A. Kitaev, AIP Conf. Proc. **1134**, 22 (2009).
[51] C.-K. Chiu, J. C. Y. Teo, A. P. Schnyder, and S. Ryu, Rev. Mod. Phys. **88**, 035005 (2016).
[52] A. P. Schnyder, S. Ryu, A. Furusaki, and A. W. W. Ludwig, Phys. Rev. B **78**, 195125 (2008).
[53] L. Fidkowski, T. S. Jackson, and I. Klich, Phys. Rev. Lett. **107**, 036601 (2011).
[54] A. Alexandradinata, X. Dai, and B. A. Bernevig, Phys. Rev. B **89**, 155114 (2014).
[55] R. B. Laughlin, Phys. Rev. B **23**, 5632 (1981).
[56] B. I. Halperin, Phys. Rev. B **25**, 2185 (1982).
[57] Y. Hatsugai, Phys. Rev. Lett. **71**, 3697 (1993).
[58] Y. Hatsugai, Phys. Rev. B **48**, 11851 (1993).
[59] X.-L. Qi, Y.-S. Wu, and S.-C. Zhang, Phys. Rev. B **74**, 045125 (2006).
[60] T. Fukui, K. Shiozaki, T. Fujiwara, and S. Fujimoto, J. Phys. Soc. Jpn. **81**, 114602 (2012).
[61] M. Sato and Y. Ando, Rep. Prog. Phys. **80**, 076501 (2017).
[62] See Supplemental Material at http://link.aps.org/supplemental/10.1103/PhysRevLett.126.067001 for more details on the mean-field theory, calculation of topological invariants, discussion on the FFLO phase, discussion on the stability of the mean-field ground state against fluctuations, and the first-principle study on a double perovskite material $SrLaVMoO_6$, which includes Refs. [63–74].
[63] A. Altland and B. D. Simons, *Condensed Matter Field Theory* (Cambridge University Press, Cambridge, England, 2010).
[64] A. B. Bernevig and T. L. Hughes, *Topological Insulators and Topological Superconductors* (Princeton University Press, Princeton, 2013).
[65] A. Skurativska, T. Neupert, and M. H. Fischer, Phys. Rev. Research **2**, 013064 (2020).
[66] Y. Yanase, T. Jujo, T. Nomura, H. Ikeda, T. Hotta, and K. Yamada, Phys. Rep. **387**, 1 (2003).
[67] H.-T. Jeng and G. Y. Guo, Phys. Rev. B **67**, 094438 (2003).
[68] J. Androulakis, N. Katsarakis, and J. Giapintzakis, Solid State Commun. **124**, 77 (2002).
[69] P. Sanyal, A. Halder, L. Si, M. Wallerberger, K. Held, and T. Saha-Dasgupta, Phys. Rev. B **94**, 035132 (2016).
[70] M. Uehara, M. Yamada, and Y. Kimishima, Solid State Commun. **129**, 385 (2004).
[71] G. Kresse and J. Furthmuller, Phys. Rev. B **54**, 11169 (1996).
[72] G. Kresse and D. Joubert, Phys. Rev. B **59**, 1758 (1999).
[73] J. P. Perdew, K. Burke, and M. Ernzerhof, Phys. Rev. Lett. **77**, 3865 (1996).
[74] S. L. Dudarev, G. A. Botton, S. Y. Savrasov, C. J. Humphreys, and A. P. Sutton, Phys. Rev. B **57**, 1505 (1998).
[75] E. Khalaf, Phys. Rev. B **97**, 205136 (2018).
[76] J. Ahn and B.-J. Yang, Phys. Rev. Research **2**, 012060(R) (2020).
[77] Y. Hwang, J. Ahn, and B.-J. Yang, Phys. Rev. B **100**, 205126 (2019).
[78] T. Saha-Dasgupta, Mater. Res. Express **7**, 014003 (2020).
[79] W. E. Pickett, Phys. Rev. B **57**, 10613 (1998).
[80] J. H. Park, S. K. Kwon, and B. I. Min, Phys. Rev. B **65**, 174401 (2002).
[81] V. Pardo and W. E. Pickett, Phys. Rev. B **80**, 054415 (2009).
[82] H. Gotoh, Y. Takeda, H. Asano, J. Zhong, A. Rajanikanth, and K. Hono, Appl. Phys. Express **2**, 013001 (2009).
[83] H. Asano, H. Gotoh, H. Matsushima, Y. Takeda, J. Zhong, A. Rajanikanth, and K. Hono, J. Phys. **200**, 052001 (2010).
[84] H. Matsushima, H. Gotoh, T. Miyawaki, K. Ueda, and H. Asano, J. Appl. Phys. **109**, 07E321 (2011).
[85] K-I. Kobayashi, T. Kimura, H. Sawada, K. Terakura, and Y. Tokura, Nature (London) **395**, 677 (1998).
[86] P. Sanyal, H. Das, and T. Saha-Dasgupta, Phys. Rev. B **80**, 224412 (2009).
[87] B. A. Connor L. Leppert M. D. Smith J. B. Neaton and H. I. Karunadasa, J. Am. Chem. Soc. **140**, 5235 (2018).
[88] S. Sumita and Y. Yanase, Phys. Rev. B **97**, 134512 (2018).